Bacterial Actin MreB as a new antibiotic target

Emőke Bódis[1], Beáta Longauer[1], András Lukács[1], Tamás Huber[1], Miklós Nyitrai[1], Géza Makkai[2], Tibor Jánosi[2], Rita Börzsei[3], Csaba Hetényi[3], Zoltán Gazdag[4], and Szilvia Barkó[1]*

[1] *Department of Biophysics, Medical School, University of Pécs, Pécs, H-7624, Hungary*

[2]*Nano-Bio-Imaging Core Facility, Medical School, University of Pécs, Pécs, H-7624, Hungary*

[3]*Department of Pharmacology and Pharmacotherapy, Pharmacoinformatics Unit Medical School, University of Pécs, Pécs, H-7624, Hungary*

[4]*Department of Molecular Biology and Microbiology Faculty of Sciences, University of Pécs, Pécs, H-7624, Hungary*

*** Correspondence:**
Corresponding Author
szilvia.barko@aok.pte.hu

Keywords: A22, MIC, MreB cytoskeleton, spectroscopy, Structured Illumination Microscope, Synergism, Vancomycin

Abstract

Actin homologue MreB has a crucial role in the synthesis of the bacterial cell wall. Disruption of the MreB filament network results in the disruption of the cell wall, which serves thus an unconventional antibacterial strategy. A22, a small inhibitor molecule binds directly to the MreB filament altering its structure causing a morphological change of the cell, leading to cell death. This effective antibacterial property is shadowed by the fact that at high concentration A22 is toxic to the eukaryotic host cells, so it cannot be administered at higher doses.

Vancomycin is a widely used antibiotic targeting the Gram-positive bacteria at concentrations as high as 10–20 μg/ml, which can occasionally cause serious side effects. Here, we present our recent findings that a synergistic interaction exists between A22 and vancomycin, which results in the inhibition of cell proliferation by the combined use of very low concentrations of A22 (6.25 μg/ml) and vancomycin (1.56 μg/ml). In addition, in the presence of A22, vancomycin is effective not only against Gram-positive bacteria, but also against Gram-negative bacteria. Since five of the seven most common antibiotic-resistant bacteria according to the WHO are Gram-negative, this synergism between A22 and vancomycin opens a new way combating bacterial infections. Our spectroscopic results support that vancomycin binds directly to MreB; using computer docking method we determined the possible binding site of vancomycin on MreB filament. This newly identified interaction between vancomycin and A22 highlights the potential of the combined use opening a new strategy to tackle antibiotic resistance.

1 Introduction

Actin homolog bacterial MreB has a fundamental role in the formation of the cell wall and maintaining basic cellular functions, like cell division, chromosome segregation, cell wall polarity and cell wall morphogenesis (White and Gober, 2012; Strahl et al., 2014). Even though the structure of the monomeric MreB shows strong similarity to that of eukaryotic actin, the two filaments differ greatly from each other. While actin protofilaments are parallel and twisted, MreB filaments are antiparallel and straight (Ent et al., 2014). Gram-positive bacteria have multiple MreB homologues, while Gram-negative bacteria have a single *mreB* gene; therefore, the knockout of MreB function could be lethal for Gram-negative bacteria (Levin et al., 1992; Varley and Stewart, 1992). This is the reason, that an increasing number of publications aiming MreB as a potential therapeutic target (Awuni, 2020; Bryan et al., 2022; Sagong et al., 2022). The fact that actin and MreB have different filamental structures could be a significant advantage in the fight against pathogenic bacteria. It becomes possible to develop specific bacterial inhibitors that do not have any toxic effect on mammalian cells.

A22 (S-(3,4-dichlorobenzyl) isothiourea) has been found as a toxin specifically against MreB, which can be applied exclusively to Gram-negative bacteria (Bean et al., 2009). The binding site of A22 is adjacent to the nucleotide binding site thus A22 binding can block the release of P_i from the ATP binding pocket resulting in destabilization of the filament (Awuni et al., 2016). Without proper ATP binding and hydrolysis, MreB cannot maintain the necessary structure required for polymerisation. Although toxicity of A22 in eukaryotic cells has been reported, severe contradictions can be found in the literature regarding the mechanism and required concentrations. It was proved that A22 can bind directly to actin, which affects cell growth and shows cytotoxic effect. It is also reported that different cell types react with varying sensitivity to the presence of A22. For example, A22 shows minimal cytotoxic activity against peripheral blood mononuclear cells (Bonez et al., 2016; Kotzialampou et al., 2021), but it is toxic for glioblastoma cell lines (Kumar et al., 2024). Since the mechanism of action of A22 would open up novel paths against pathogenic bacteria, intensive research is being launched in this area (Muheim et al., 2017; Kumar et al., 2024), even in case of multidrug resistant bacteria (Nicholson et al., 2012).

A combination of different antibacterial agents, e.g., use of clinical antibiotics with anti-MreB compounds or the use of adjuvants, can be the direction to tackle the growing problem of multidrug resistance. One very beneficial approach is to use different antibiotics in combination with A22 to achieve greater antibacterial efficacy (Kotzialampou et al., 2021) through destroying MreB filamental structure, which has a multifunctional character and therefore is essential for bacterial viability. For example, synergism occurred in the case of A22-cefoxitin and A22-azithromycin against *E. coli* (Kotzialampou et al., 2021). This synergistic effect has not yet been tested and described for dual A22-vancomycin use.

Vancomycin is an antibiotic used to treat Gram-positive bacterial infections. This tricyclic glycopeptide inhibits cell wall formation in streptococci, enterococci and staphylococci (Kang and Park, 2015). To achieve optimal results when administering vancomycin to patients, dosage adjustment is based on patient-specific factors. Typical dosage is 125 mg-1 g in vial as recommended by the WHO (World Health Organization, 2025). Intravenous vancomycin dosing typically achieves steady-state trough serum concentrations of approximately 10–20 μg/ml in adults with normal renal function (James and Gurk-Turner, 2001a; Kitzis and Goldstein, 2006; Perin et al., 2020; INTRAVENOUS VANCOMYCIN DOSING AND MONITORING GUIDELINES, n.d.). In the case of infections caused by Gram-negative bacteria, vancomycin treatment is not considered, as the minimum inhibitory concentration of vancomycin is much higher for Gram-negative bacteria (200-250 μg/ml). Even

vancomycin-resistant strains have a much lower MIC value (8μg/ml, VRSA). The side effects of vancomycin (hypersensitivity reactions, nephrotoxicity, ototoxicity) occur even at the indicated concentration, so it is not possible to increase the dose further.

Our experiments show however, when the MreB inhibitor A22 is used in combination with vancomycin, the resulting powerful synergy causes the MIC value of Gram-negative bacteria to reach that of Gram-positive bacteria. In other words, in this sense, A22 makes Gram-negative bacteria "Gram-positive-like" in terms of their resistance to vancomycin.

The ESKAPEE group is an acronym for antibiotic-resistant bacteria responsible for hospital-acquired infections (Krul et al., 2025). They pose the greatest threat to global health and healthcare systems because they are difficult to treat and, due to their resistance, are becoming increasingly resistant to drugs. The members of the group (*Enterococcus faecium*, *Staphylococcus aureus*, *Klebsiella pneumoniae*, *Acinetobacter baumannii*, *Pseudomonas aeruginosa*, *Enterobacter species* and *Escherichia coli) (*except for the first two) are Gram-negative, for which vancomycin treatment based on the synergism with A22 may be an effective tool.

As we mentioned, the synergistic effect observed with the combined use of A22 and vancomycin has not yet been described. Our results based on microbiological and microscopic observations suggest that. Furthermore, we also confirmed that vancomycin binds directly to the MreB protein *in vivo* and presumably induces structural changes in it. This statement was further strengthened by finding the putative binding sites of vancomycin on MreB by molecular docking calculations. Our findings may provide a basis for research aimed at developing drugs – through the combined action of one or even several antibiotics – that inhibit bacterial growth by blocking the function of the MreB protein, especially in Gram-negative infections.

Materials and methods

2.1. Determination of minimum inhibitory concentration (MIC) and synergism (FICI)

Minimal inhibitory concentration (MIC) values were determined according to the Clinical and Laboratory Standards Institute (CLSI) M07-A9 broth microdilution method ((Clinical and Laboratory Standards Institute, 2015)). The A22 was dissolved in DMSO, and the vancomycin was dissolved in distilled water. The antibacterial agents were tested on a 96-well plate in two-fold serial dilutions ranging from 0.78 to 400 μg ml^{-1} for vancomycin and 1.56 to 200 μg ml^{-1} for A22. Final solvent concentrations for each treatment were 1% (v/v). The optical density of the bacterial suspension was set to 0.12 (OD_{625}, McFarland standard 0.5), and a 500-fold dilution with LB nutrient solution was used to obtain a concentration of $2 \cdot 10^5$ cells/ml. The results were evaluated after 24 hours of incubation at 37 °C. Following treatment, cell densities were measured by Multiskan EX 355 (Thermo Electron Corporation) spectrophotometer on a 594 nm wavelength. Evaluation of 80% inhibitory effects (MIC_{80}) of antibacterial agents were applied and compared to antibacterial agent-free controls. Each treatment was performed in triplicates.

The interaction between vancomycin and A22 on the *E. coli* K12 strain was examined with the chequerboard broth microdilution method. Sample preparation for microdilution was performed according to the antibacterial susceptibility method as described above. The antibacterial agent's interaction types were determined based on the fractional inhibitory concentration index (FICI) calculated according to Nyilasi et al. (Nyilasi et al., 2014). Using the smallest MIC value of the antimicrobial agents, the value of the fractional inhibitory concentration index, i.e., ΣFICI (fractional

inhibitory concentration index), was calculated using the formula below. If ΣFICI≤0.5, this implies synergism, and the two antibacterial agents support the effect of each other.

$$\Sigma FICI = \frac{MIC_{A,together}}{MIC_{A,itself}} + \frac{MIC_{B,together}}{MIC_{B,itself}} \qquad \text{Eq.1}$$

2.2. Examination of the growth curve

E. coli K12 cell culture (Sigma-Aldrich) was grown overnight in Luria Broth (0.5% yeast extract, 1% NaCl, 1% peptone) nutrient solution at 37 °C in a shaking incubator. The next day, in the absence or presence of 1.56 µg/ml vancomycin and/or 6.25 µg/ml A22, 100-fold dilution of bacterial culture was made, which were grown in 5 ml of fresh nutrient solution. The optical density of the cells was detected repeatedly at 600 nm on a Perkin Elmer Lambda XLS+ spectrophotometer. Above OD 0.5 dilution was applied for determining OD of cultures, and calculated OD was plotted on graph.

2.3. Visualization of Bodipy-vancomycin uptake in *E. coli* cells

E. coli K12 cells were grown overnight at 37 °C in LB medium in a shaking incubator. The next day a new culture was established by this source, making a 100-fold dilution. Additionally, a 2% agarose pad was made by dissolving 2g agarose in a 100 ml LB medium. Agarose was dissolved by heating in a microwave for 30-60 seconds. Then 100 µg/ml vancomycin or 27 µg/ml A22, none of them or both were given to the fluid agarose. 1µg/ml Bodipy-vancomycin was applied by every sample. When the agarose was solidified on the coverslip, and the cultures achieved the logarithmic phase after 200 minutes, the cells were smeared on agarose pad. After an additional two hours incubation period, the cells were visualized using an Olympus IX81 microscope. The percentage of cells that have taken up Bodipy-vancomycin was determined by combining the transmission and fluorescence images. The percentages of cultures containing either vancomycin or vancomycin and A22 were subjected to a t-test to determine whether the difference was significant in response to A22 treatment.

2.4. Fluorescence microscopy observations

E. coli K12 cells were grown for three hours as described above (see "*Examination of the growth curve"* section). The cells were harvested by centrifugation at 13000 rpm, 22°C, 1 minute. After washing in PBS, the pellet was resuspended in paraformaldehyde solution (4%) and it was stored at room temperature for 10 minutes. After a washing step the samples were labelled with Bodipy-vancomycin (1 µM=1.49 µg/ml). The cells were centrifuged and after a washing step in PBS they were applied on poly-L-lysine coated coverslip. The cells were visualised with Zeiss Elyra S1 SIM microscope, the pictures were analysed using Fiji Software.

2.5. Investigation of binding between *Tm*-MreB and Bodipy-vancomycin

Expression and purification of *Thermotoga maritima* MreB (*Tm*-MreB) protein was achieved as described earlier (Longauer et al., 2022).

2.6. Steady-state anisotropy measurements

The steady-state anisotropy measurements were performed on a Jobin Yvon Horiba fluorimeter. 1 μM fluorescently labelled vancomycin (Invitrogen) (BODIPY^{TM} FL Vancomycin, FLV) was used to test binding, and the protein concentration gradually increased from 1 μM to 60 μM. Our test was performed with 0.2 mM ATP and/or polymerizing salt (100 mM KCl and 2mM $MgCl_2$). The following equation was used to determine the binding affinity of Bodipy-vancomycin to *Tm*-MreB:

$$y = \frac{y_{min}+((y_{max}-y_{min})*\left(\left((KD+FLV+x)-(((KD+FLV+x)^2\right)-(4*FLV*x))^{0,5}\right)\right)}{(2*FLV)} \quad \text{Eq.2}$$

In this equation, the following values were used: x (*Tm*-MreB concentration), y_{min} (the lowest fluorescence anisotropy value), y_{max} (the highest saturation fluorescence anisotropy value), FLV (the concentration of fluorescent vancomycin), and KD (the binding constant).

2.7. Sedimentation assay

20 μM *Tm*-MreB was incubated overnight at 4° C in the presence (100 μg/ml) or absence of unlabelled vancomycin. The next day the samples were ultracentrifuged at 100,000 g at 22° C for 30 minutes. The pellets and supernatants were analysed by 10% SDS-PAGE.

2.8. Labelling of *Tm*-MreB with Bodipy-vancomycin

20 μM of *Thermotoga maritima* MreB (*Tm*-MreB) was incubated for two hours with 1 μM (=1,45 μg/ml) of Bodipy-vancomycin in the presence or absence of 100 μg/ml of native vancomycin. Samples were then dropped onto coverslips and examined at 100x magnification using an Olympus IX 81 fluorescence microscope.

2.9. Structural calculations

2.9.1. Target preparation. The apo structure of *Tm*-MreB protein (PDB code: 1jce, (Ent et al., 2001)) was obtained from the PDB Database (Berman et al., 2000). Water molecules were deleted, hydrogens were added to the structure, and the N-terminal of the protein was neutralized by capping with the methyl-acetate group (ACE). This structure was used as ligand-free (apo) monomeric *Tm*-MreB. Symmetry mates of the apo *Tm*-MreB was generated by PyMol (Schrödinger, LLC, 2015) to use the dimer linear structure (Ent et al., 2001) for calculations.

2.9.2. Ligand preparation. The crystal structure of vancomycin dimer was obtained from the PDB Database (PDB code: 1sho, (Schäfer et al., 1996)). Water and ion molecules were cut, and hydrogens were added to the structure. The molecule was energy-minimized using the semi-empirical quantum chemistry program package, MOPAC (Stewart, 2013), with PM7 parametrization (Stewart, 2013). The minimized monomeric form was used for docking calculations.

2.9.3. Vancomycin dimer. The minimized crystallographic dimeric vancomycin (PDB code: 1sho, (Schäfer et al., 1996)) was superimposed to the representative monomer conformation (rank 1) docked to the dimer target structure using the pair fitting module of PyMol (Schrödinger, LLC, 2015), resulting in 0.377 Cα RMSD. The pdbqt files for the representative docked monomeric and the opposite partner of the aligned dimeric structures were prepared by Autodock Tools (Morris et al., 2009) using torsion restraints. The pdbqt files were merged to produce the dimeric vancomycin in pbdqt format. This dimeric ligand structure was used in docking calculations.

2.9.4. Docking calculations. The minimized and aligned vancomycin ligands were submitted to docking calculations using Autodock 4 (Morris et al., 2009). Gasteiger-Marsilli partial charges were assigned both to the ligand and MreB target structures in AutoDock Tools (Morris et al., 2009), and united atom representation was applied for non-polar moieties. In all calculations, targets were treated rigidly. Flexibility was allowed at all active torsions of monomeric vancomycin; however, torsion restraints was applied on its dimeric form. Grid maps were prepared by AutoGrid4 (Morris et al., 2009) centred to 27.99, 20.69, 21.15 and 31.99, 24.69, 21.15 with 100x100x100 and 126x126x126 grid points at a 0.375 Å spacing for monomeric and dimeric *Tm*-MreBs, respectively. Lamarckian genetic algorithm was used for global search in 100 docking runs covering both the dimerization interface (Ent et al., 2001) and ATP binding site (Ent et al., 2001). Docked ligand conformations were ranked based on the corresponding calculated target-ligand intermolecular interaction energy (E_{inter}) values and subsequently clustered using a root mean squared deviation (RMSD) tolerance of 3.5 Å between the cluster members. E_{inter} is the sum of van der Waals, H-bond, desolvation and electrostatic interaction energies (Huey et al., 2007). Conformations were selected and studied further based on the docking locations and interaction energy values (i.e., rank 1, rank 2, rank 22 and rank 52).

2.9.5. Calculation of stabilizing energy contribution of vancomycin for Tm-MreB dimerization. Vancomycin's role for *Tm*-MreB dimerization was also examined from the point of energetical view. E_{inter} values between the MreB monomers were calculated by using the "epdb" keyword in the dpf file of Autodock (Huey et al., 2007). Firstly, E_{inter} was calculated between two vancomycin-free *Tm*-MreB monomer units and named as E_{dimer}(apo). Secondly, E_{inter} was also calculated between vancomycin-bound *Tm*-MreB monomer unit and a vancomycin-free *Tm*-MreB monomer unit, and it was named E_{dimer}(holo). The stabilizing effect of vancomycin on the dimerization of *Tm*-MreB monomer units was expressed as a stabilizing energy contribution of vancomycin (E_{st}) using the percentage of E_{inter}(apo) calculated by Equation 3. E_{st} shows the energy gain of *Tm*-MreB dimerization in the presence of vancomycin compared to the absence of it expressed in percentage.

$$E_{st} = \frac{E_{dimer}(holo) - E_{dimer}(apo)}{E_{dimer}(apo)} \times 100\ \% \qquad \text{Eq. 3}$$

Results

The aim of this study was to investigate the presumed synergistic effect of the antibiotics A22 and vancomycin on the MreB filaments inside the *E. coli* cells and to determine how much they can enhance each other's inhibitory effect as inferred from growth rate measurements. We also provide applicable concentrations of the antibiotics considering their synergistic effect. To determine the most probable binding site of these antibiotics, *in silico* docking calculations were made. Besides, using fluorescence spectroscopy and microscopy techniques, we give strong evidence for direct binding of vancomycin to MreB filaments.

3.1. Measurements on *E. coli* cells

3.1.1. Microbiological FICI assay

Microbiological assays were used to determine the MIC_{80} (minimum inhibitory concentration) value of the two antimicrobials, which is the lowest concentration at which growth inhibition of more than 80 % is observed. The synergistic effect between the two agents was detected by a checkerboard microdilution test, where FICI (fractional inhibitory concentration index) values under 0.5 represent synergism.

Based on our earlier microbiological data, our aim was to determine the lowest concentration of A22 and vancomycin, which synergistically inhibits bacterial growth of *E. coli* (Table 1). For this one, in a 96-well plate various concentration of A22 (1.56-200 μg/ml) and vancomycin (0.78-400 μg/ml) was added to $2 \cdot 10^5$ cells/ml solution. As a control, cell growth inhibition was determined by A22 and vancomycin separately and in the absence of both. The inhibitory concentration in case of A22 and vancomycin was 100 μg/ml and 200 μg/ml, respectively. If the combination of A22 and vancomycin was applied, the cell growth inhibition was observed in the range of 6.25-25 μg/ml and 1.56-50 μg/ml, respectively (Table 1). Another method to prove synergism between the two agents is to keep one of the agents constant and vary the concentration of the other ones. According to this the vancomycin inhibitory effect falls in the range of 6.25-50 μg/ml at constant 3.125 μg/ml A22 concentration (Table 1).

The synergistic effect already occurs at rather low vancomycin (1.56 μg/ml) and A22 (6.25 μg/ml) concentrations compared to the doses usually used in clinics (James and Gurk-Turner, 2001b; Martin et al., 2010; Perin et al., 2020), the combined use of an antimicrobial agent based on MreB inhibition may be suitable for Gram-negative infections.

3.1.2. Growth rate of bacterial culture assay

For the determination of the growth rate of bacterial cultures *E. coli* K12 cells were growing in the presence of 1.56 μg/ml of vancomycin and/or 6.25 μg/ml of A22 (these are the lowest synergetic inhibitory concentrations determined from the microbiological assay). As a control, cells were grown in the absence of any antibiotics (Fig 1A). Compared these values to previous literature data, this concentration of both antibiotics is far below the value that would be toxic to human cells (for A22 it is between 25-32 μg/ml (Bonez et al., 2016; Kumar et al., 2024), for vancomycin it is 2-5mg/ml (Braun et al., 2020; Hall et al., 2024)).

Our results showed that none of the antibiotics could separately inhibit growth of bacteria at these applied concentration values (Figure 1B), the tendency of the bacterial growth is not different from the untreated cells. However, using vancomycin and A22 simultaneously, a strong inhibition of bacterial growth was observed (Figure 1B, magenta symbols). Based on this observation, vancomycin and A22 demonstrate strong synergism against *E. coli* cell growth.

MIC_{80} alone (μg/ml)		MIC_{80} in combination (μg/ml)	FICI
A22 [100]	**Van** [200]	50 + 0.78	0.5
		6.25 + 1.56	0.07
		3.125 + 6.25	0.06

	1.56 + 25	0.14

Table 1. There is a synergistic effect between vancomycin and A22. *The numbers in the left column refer to the MIC values for the two compounds separately. The middle column shows the concentration ranges in which the two antibiotics must be used to achieve the synergistic effect. If one of the antibiotics is kept constant, the concentration range of the other one changes to achieve the synergistic effect. The right column shows the fractional inhibitory concentration index (FICI) values of A22 and vancomycin in different combinations. FICI values under 0.5 means that there is synergism between two compounds.*

279

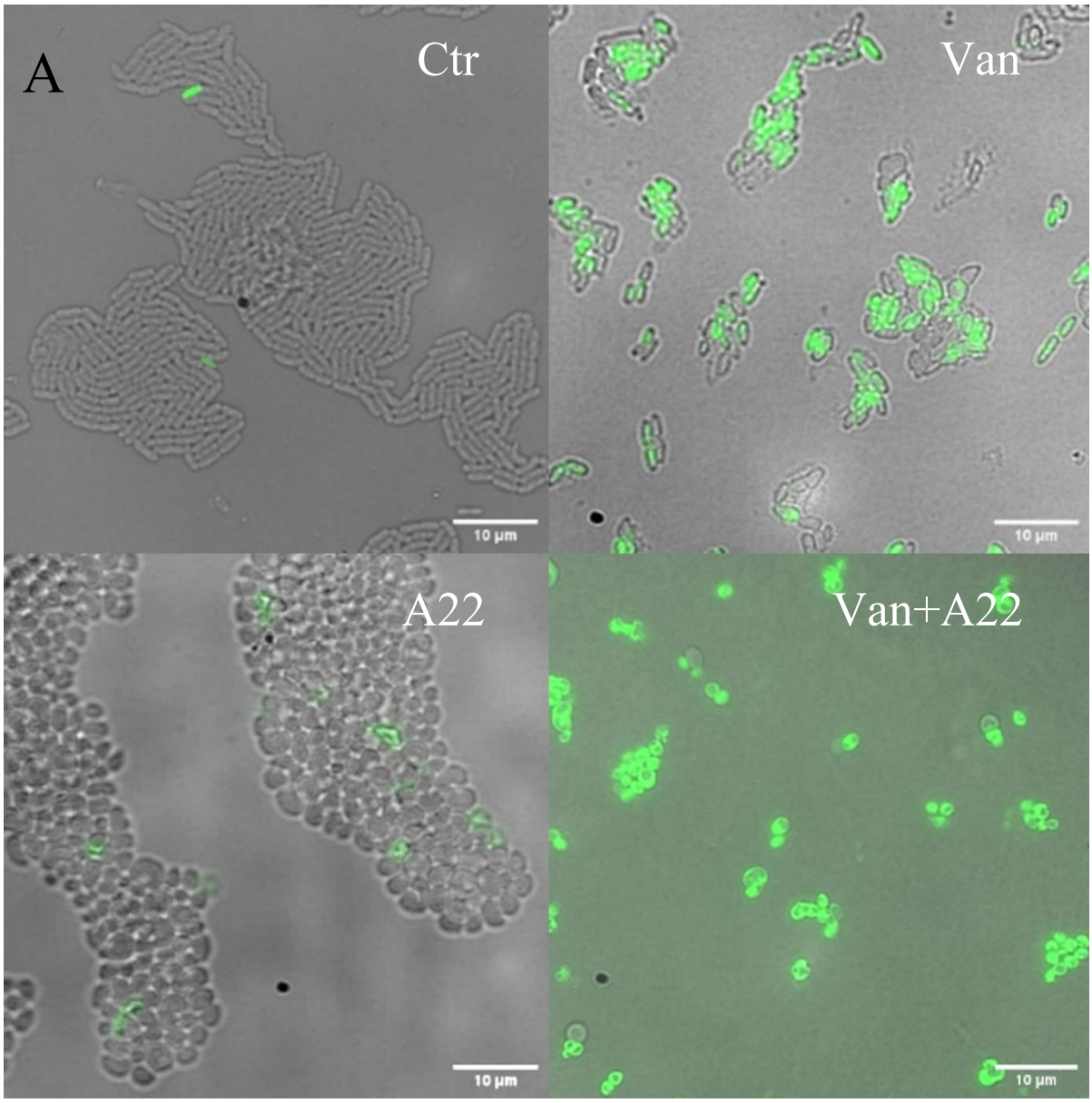
A
Ctr
Van
A22
Van+A22
10 µm

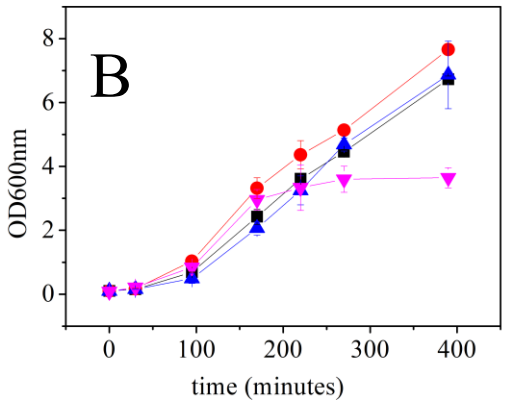
B
OD600nm
time (minutes)
0
2
4
6
8
0
100
200
300
400

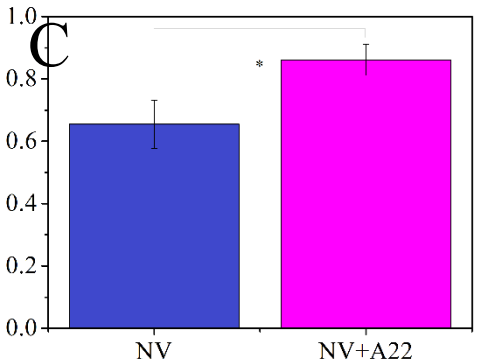
C
1.0
0.8
0.6
0.4
0.2
0.0
*
NV
NV+A22

Figure 1A: The percentage of fluorescent cells increases with vancomycin and A22. *E. coli K12 cells were grown in Bodipy-vancomycin containing agarose pad with or without 27 μg/ml A22, 100 μg/ml vancomycin, or both A22 and vancomycin in the specified amounts (ctr: control-without any antibiotics, Van: only vancomycin is present, A22: only A22 is present, Van + A22: vancomycin and A22 are both applied) . The samples were visualized with a fluorescence microscope with 100X magnification. The transmission and fluorescence pictures were merged. The unlabeled vancomycin enhances the entrance of Bodipy-vancomycin in E. coli cells, though A22 does not have this effect on its own. If A22 and vancomycin are present simultaneously, the uptake of Bodipy-vancomycin increases even more.* ***B: E. coli growth is inhibited at lowest antibiotics concentrations used in FICI assay***. *E. coli K12 cells were grown in the absence of antibiotics (black squares), in the presence of 6.25 μg/ml of A22 (red circles), 1.56 μg/ml of vancomycin (blue triangles), or both (magenta stars). In case of optical density values above 0.5 the samples were diluted for measuring and calculating their original OD. The figure shows the standard deviation based on two sets of measurements.* ***C:*** *In samples containing only vancomycin (blue column) or vancomycin and A22 (magenta column), the proportion of cells that took up fluorescent vancomycin was significantly different.*

3.1.3. Fluorescence microscopy assay of vancomycin uptake

In order to determine whether the synergetic effect between A22 and vancomycin found in the microbiological assay could be explained by an increased rate of vancomycin entry into the cells, fluorescent microscopy assays were performed. *E. coli* K12 cells were grown in the presence of Bodipy-vancomycin in the presence and absence of vancomycin and A22. The existence of Bodipy-vancomycin in the growing medium (agarose pad) is needed for visualization using a transmission and fluorescence channel. Our results showed that in control experiments (absence of A22 and vancomycin) the Bodipy-vancomycin hardly enters the cells (Figure 1C, left upper). The presence of A22 dissolved in the agarose pad does not enhance the appearance of Bodipy-vancomycin in cells (Figure 1C, left down). The presence of native vancomycin significantly facilitated the cellular uptake of Bodipy-vancomycin (Figure 1C, right upper). The cells growing on the agarose pads containing both A22 and vancomycin took up even higher proportion of Bodipy-vancomycin compared to the sample having only vancomycin or A22 (Figure 1B). To verify this observation, we performed a two-sample t-test using the percentage of labelled cells to the total number of the cells. A significant difference between the samples containing vancomycin and those containing vancomycin and A22 (Figure 1C.) was observed. This finding suggests that A22 can enhance the vancomycin penetration into bacterial cells.

3.1.4. Determination of the Bodipy-vancomycin localization in the cell

Structured Illumination Microscopy (SIM) was used to determine whether the Bodipy-vancomycin labelling pattern in *E. coli* was indeed localised intracellularly. If only the membrane or cell wall is labelled, no fluorescent labelling is expected in the cytoplasm (Figure S1). However, if MreB binds the Bodipy-vancomycin, intracellular labelling is expected. For this purpose, we examined cell membrane labelling with Nile Red fluorophore, which is known to give a signal in the apolar medium of the membrane. In this case, only the membrane gave a signal, and the interior of the cells remains unlabelled (Figure S1). Comparing the Nile Red and the Bodipy-vancomycin labelled cells difference of the spatial distribution of fluorescence is shown (Figure 2A). In the experiments where Bodipy-vancomycin was used as a fluorophore, the cytoplasm of the bacterial cells showed intense staining compared to Nile Red minimal intensity. Besides, Bodipy-vancomycin seems to label cell wall and/or cell membrane as well. From these observations, we conclude that Bodipy-vancomycin binds not only the outer part of the cell but also with higher extent to the MreB protein inside the cell.

3.1.5. Determination of the shape of the cells

A22 is a specific inhibitor of MreB; in its presence, MreB loses its function, resulting in round cells instead of rod-shaped ones. This effect depends on the concentration of the A22 and the cell division phase. Applying the lowest concentrations of A22 (6.25 μg/ml) coming from our microbiological assay, some of the cells remained rod-shaped, while others were rounded (Figure 2B). Vancomycin treatment at the lowest concentration (1.56 μg/ml) did not influence the shape of the rod-like cells, they could maintain their natural form (Figure 2C). However, when vancomycin and A22 are used simultaneously at the lowest concentrations (1.56 μg/ml and 6.25 μg/ml, respectively), all cells take on a round shape (Figure 2D). This observation also supports the earlier experiences that vancomycin enhances the destabilizing effect of A22 on MreB, which can be considered a form of synergism. In addition, in the A22 containing samples (without and with vancomycin, Figure 2B and D), when round shape of the cells develops, MreB seems to be delocalised from the membrane and appears with higher intensity in the cytoplasm. This is presumably why a gap appears between the cell wall Lipid II signal and the cytoplasmic MreB signal. Furthermore, it is also impressive that not only the shape of the cells has changed from rod-shaped to round, but also their volume has undergone significant growth. To analyse the length/width ratio (Figure 2E), the median and the ratio distribution of the control cells refers to typical rod-shaped cell population. In the presence of A22 the distribution of the length/width ratio is much wider indicating not only a rod shape but also a round shaped population of the cells are also present, the heterogeneity of the cell population is clearly seen. In case of the presence of both A22 and vancomycin, the median is close to 1 (typical for spherical cells) and the distribution of the length/width ratio is narrow, indicating a more homogenic size and shape cell population, all the cells are close to round shape.

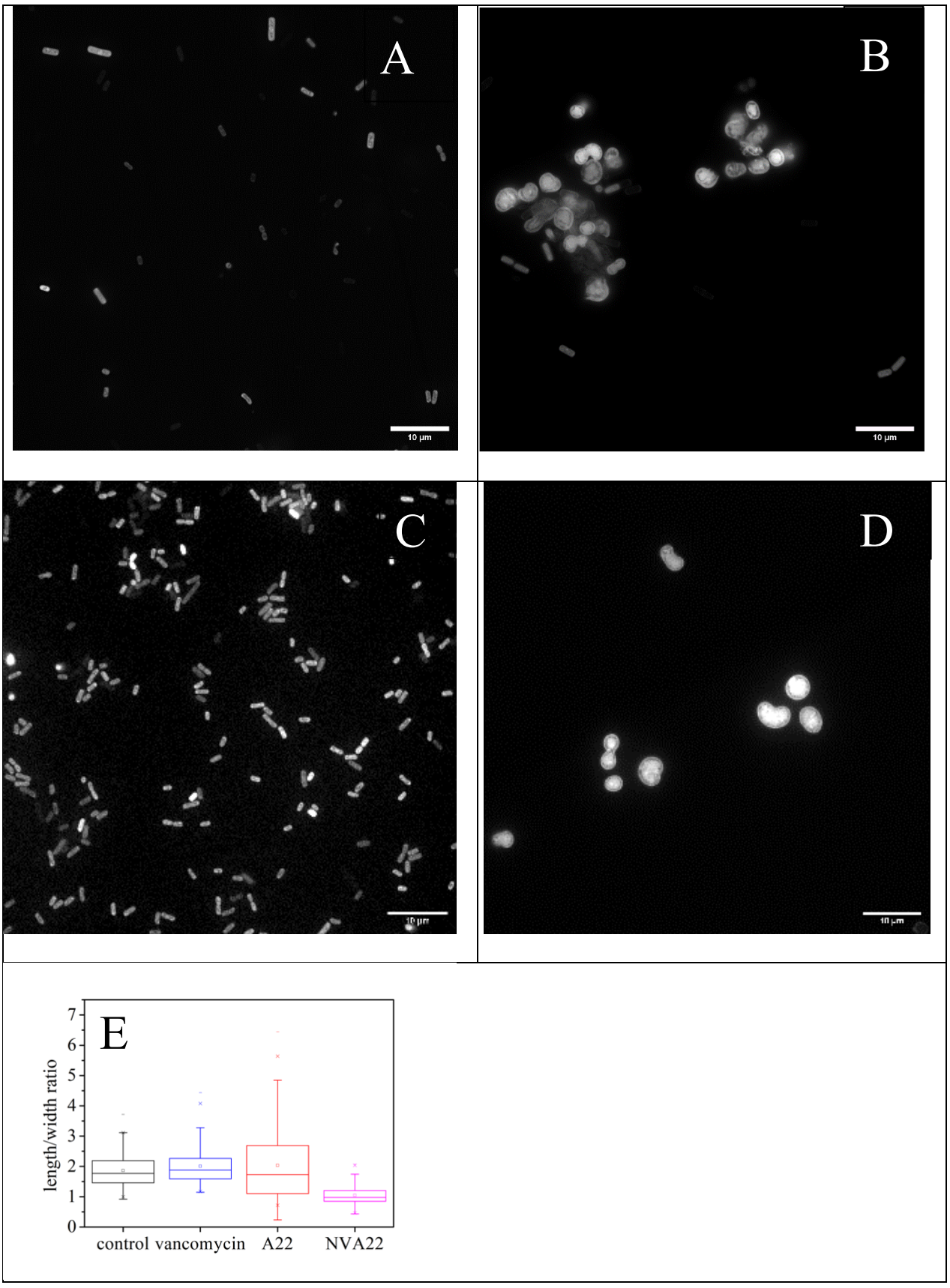

348

Figure 2. Bodipy-vancomycin labelled E.coli cells. *In all cases the cells were labelled Bodipy-vancomycin. E. coli K12 cells were labelled with Bodipy-vancomycin (A) in the absence of other antibiotics (A22, vancomycin), and the rod shape of E. coli cells was observed. (B) In the presence of A22 most of the cells become rounded, although some rod-shaped can be also observed. (C) When non-labelled vancomycin was added, the cells remain rod-shaped. (D) If non-labelled vancomycin and A22 are applied simultaneously, every cell loses its rod form. (E): Vancomycin enhances the effect of A22. The round shape forming effect of A22 is notably increased in presence of vancomycin (A22 compared to vancomycin+A22) (n=100-130).*

3.2. *In vitro* measurements on *Tm*-MreB and vancomycin complex formation

3.2.1. Fluorescence anisotropy measurements of Bodipy-vancomycin on *Tm*-MreB

To investigate the direct vancomycin-MreB binding, we measured the steady-state fluorescence anisotropy and fluorescence intensity of Bodipy-vancomycin in the presence of the expressed *Thermotoga maritima*-MreB (*Tm*-MreB). The results of the steady-state anisotropy measurements show that Bodipy-vancomycin binds to *Tm*-MreB in a concentration-dependent manner (Figure 3A), the calculated binding constant in Buffer A (4 mM Tris-HCl, pH = 8.0, 0.1 mM $CaCl_2$) was found K_d = 8.33 ± 0.57 μM. Further we calculated the binding affinity of Bodipy-vancomycin with *Tm*-MreB at different buffer conditions (Table S1). The binding constant in the presence of ATP (0.2 mM), high KCl (100 mM) and both of them slightly changed, K_d = 6.89 ± 0.51 μM, K_d = 5.59 ± 1.21 μM and K_d = 4.05 ± 0.72 μM , respectively, meaning the binding is the strongest when nucleotide is present and the salt concentration is closer to physiological conditions (Table S1).

The direct binding between *Tm*-MreB protein and vancomycin was also confirmed by our additional spectroscopic measurements, such as (i) the shift in the fluorescence emission maximum of Bodipy-vancomycin upon *Tm*-MreB binding (Figure S2), (ii) the increment of steady-state anisotropy value of Bodipy-vancomycin upon addition of non-labelled vancomycin (Figure S3), and (iii) the change in the fluorescence of *Tm*-MreB tryptophan upon the addition of non-labeled vancomycin (Figure S4).

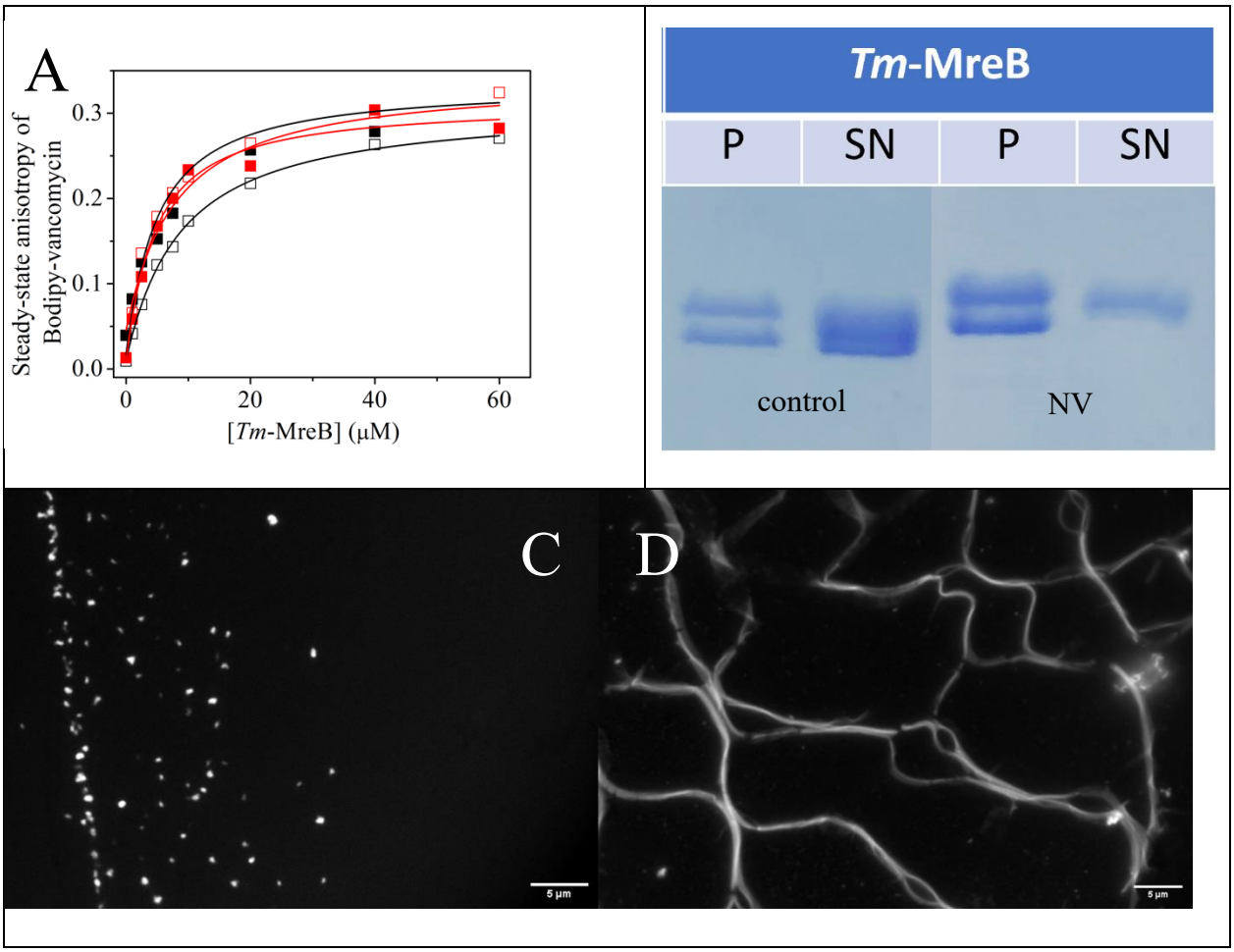

Figure 3. Vancomycin binds directly Tm-MreB and forms bundles. A. Tm-MreB binding increases the steady-state anisotropy of Bodipy-vancomycin. *1 μM Bodipy-vancomycin was incubated with Tm-MreB in various concentrations and the steady-state anisotropy of each sample was measured. Black squares (buffer A), red squares (buffer A in presence of polymerization salt), filled squares (in the presence of 0.2 mM ATP, and unfilled squares (in the absence of ATP). Bodipy-vancomycin binds Tm-MreB in any buffer conditions with similar affinities.* ***B. Vancomycin stabilises interfilamental connections between adjacent MreB molecules.*** *Vancomycin (NV=non-labelled vancomycin) tends to form MreB bundles that can be sedimented by ultracentrifugation. Therefore, the amount of Tm-MreB increased in the pellet (P) in the presence of NV.* ***C and D: Bodipy-vancomycin labels Tm-MreB and native vancomycin forms MreB bundles in fluorescence microscope*** *(Bodipy-vancomycin labelled Tm-MreB filaments in the absence (C) or presence (D) of vancomycin.*

3.2.2. SDS-PAGE measurements of the binding of Bodipy-vancomycin on *Tm*-MreB

To describe, whether vancomycin can induce a conformational change on *Tm*-MreB, altering the filament structure, sedimentation experiments were performed. 20 μM of *Tm*-MreB was incubated overnight with vancomycin in 150 μg/ml concentration. *Tm*-MreB in the presence and absence of

vancomycin (Figure 3B) were centrifuged and analysed by SDS-PAGE. A significant increase in the amount of pellet (P) was observed in the presence of vancomycin (Figure 3B), indicating that vancomycin binding strengthens the intermolecular connection between *Tm*-MreB monomers, without knowing the exact inter- and/or intramolecular modifications.

3.2.3. Fluorescence microscopy measurements of the binding of Bodipy-vancomycin on *Tm*-MreB

Under SIM microscope the structural differences between the *Tm*-MreB (20 μM) saturated with vancomycin (100 μg/ml) was compared to *Tm*-MreB itself. To visualise the structure of the filaments, 1μg/ml Bodipy-Vancomycin was applied (Figure 3C and 3D). The images clearly show a remarkable structural difference ascribed to the effect caused vancomycin binding. This finding confirms the result of the sedimentation experiment.

3.3. Docking calculations support binding between vancomycin and Tm-MreB

To support our experimental results, we performed *in silico* docking calculations. Both the monomeric and dimeric forms of vancomycin were docked to a representative unit of the *Tm*-MreB filament (target). The target was either a monomeric or a dimeric form of the *Tm*-MreB. The search area included both the dimerization interface (Ent et al., 2001) and ATP binding pocket (Ent et al., 2001). One hundred docking runs were performed in all cases, and they resulted in two main sites located in the dimerization interface (Figure 4**)**. The corresponding target-ligand interaction energy (E_{inter}) values were calculated and listed in Table S3.

The monomeric form of vancomycin tends to dock to Site 1 with the best E_{inter} in the cases of both (monomeric and dimeric target) forms of *Tm*-MreB. Docking calculations to the monomeric and dimeric *Tm*-MreB also revealed the same binding conformations of the monomeric vancomycin both on Site 1 and Site 2; however, they were not the best energy poses on the dimeric *Tm*-MreB (Table S2 and S5). As Figure 4 illustrates, vancomycin could play a stabilizing and bridging role between the *Tm*-MreB monomer units. The close-up view illustrates that in Site 1 and Site 2 the main stabilizing interactions in vancomycin positions of the best E_{inter} include H-bonds with target residues M1:A61 and M2:E266 in Site 1, and M1:K49 and M2:E145 in Site 2 (Figure 4C) that may be good candidates for future site-directed mutagenesis experiments.

.

At the same time, the dimeric vancomycin prefers Site 2 and shows a comparably good E_{inter} as it was observed at Site 1 (Table S2). However, vancomycin still forms a bridge between the monomer *Tm*-MreB units and, therefore, it could maintain its stabilizing role (Figure 4, Figure 5). To quantify the stabilizing role of vancomycin, a stabilizing energy contribution of vancomycin was calculated (E_{st}, Methods). E_{st} accounts for the energy gain corresponding to the presence of vancomycin during *Tm*-MreB dimerization (Figure 6, Table S3). The binding of both vancomycin monomeric and dimeric forms increased the E_{st} between the monomeric *Tm*-MreB units by at least 27% (Figure 5A). Therefore, it can be concluded that vancomycin may enhance *Tm*-MreB dimerization (Figure 5B).

A22 has an experimental complex structure with ADP and MreB (*Caulobacter vibrioides*). MreB sequences of *Thermotoga maritima* and *Caulobacter vibrioides* are in 52% identical the RMSD of the ADP- as well as A22-binding sites show minimal difference, 0.668 Å and 1.652 Å, respectively. Vancomycin binding sites (neither Site1 nor Site2) did not overlap with either A22 or ADP (nucleotide) binding pocket after the superposition of MreB-ADP-A22 complex to MreB-vancomycin structure. This finding supports our experimental results that vancomycin can bind to MreB even in the presence of both ADP and A22, so there is no structural barrier/obstacle for the synergistic effect of A22 and vancomycin on MreB function.

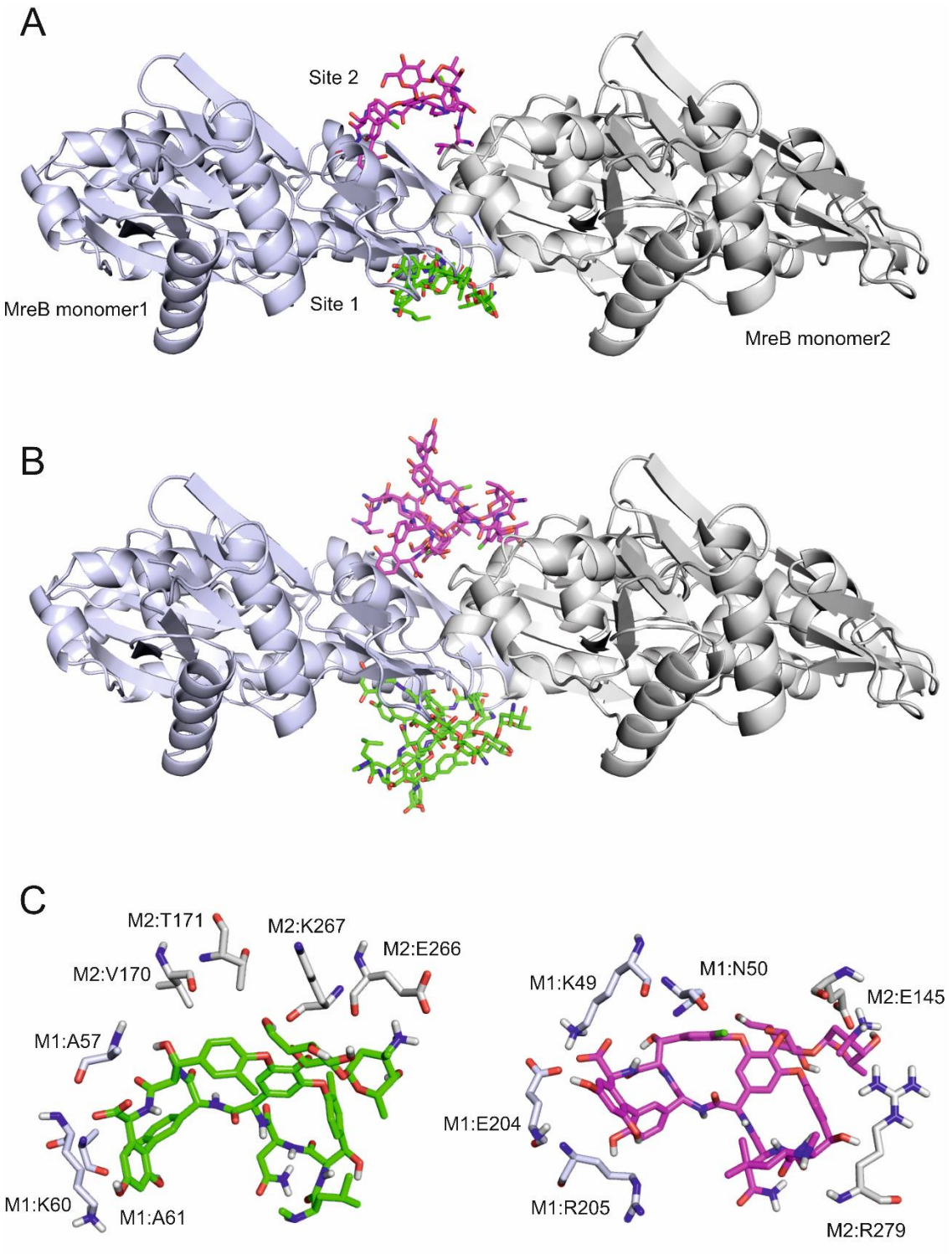

439

440

441 **Figure 4. The vancomycin molecule has two binding sites on MreB. A) The structure of monomeric**
442 **vancomycin molecules bound (sticks, rank1: green, rank 22: magenta) to Site 1 (down) and Site 2 (up) of**
443 **the dimeric MreB filament (cartoon, monomer1: bluewhite, monomer2: gray). B) The structure of**
444 **dimeric vancomycin molecules bound (sticks, rank1: magenta. rank2: green) to Site 1 (down) and Site 2**
445 **(up) of the dimeric MreB filament (cartoon, monomer1: bluewhite, monomer2: gray). C) The close-up**

view of monomeric vancomycin bound to Site 1 and Site 2 of the dimeric MreB filaments, showing the target residues interacting with vancomycin (sticks, on Site 1: green, on Site 2: magenta) within 3.5 Å distance.

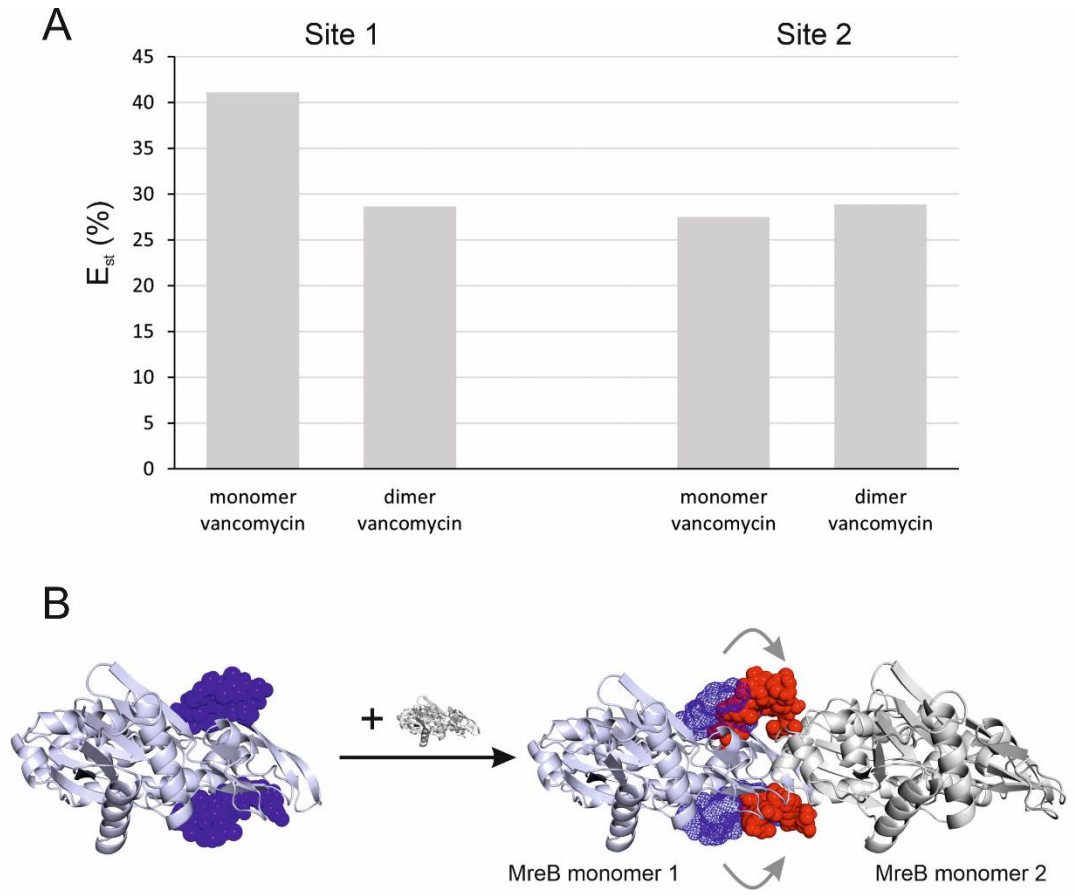

Figure 5. (A) The stabilization effect of vancomycin on the MreB-MreB interaction expressed as Est (Eq. 3, Methods) on Site 1 and Site 2, respectively. (B) The role of vancomycin assisting MreB dimerization. *Monomeric vancomycin (blue, spheres) bound to Site 1 and Site 2 of MreB monomer1 (bluewhite, cartoon) may assist the linking of MreB monomer2 (gray, cartoon) and move to a bridging position (red, spheres) to stabilize the dimerized MreB units. Gray arrows represent the relocation and repositioning of monomeric vancomycin.*

The synergistic effect between the two substances was thus confirmed in diverse ways: inhibition of cell proliferation, a drastic reduction in the minimum inhibitory concentration, and changes in cell morphology.

4. Discussion

Over the last couple of decades, the danger of bacterial infections has intensified due to the rapid increase of antibiotic resistance. The widespread use of antibiotics and the constant modifications of antibacterial agents have failed to result in a breakthrough; therefore, the discovery of new antimicrobial pathways is crucial. The bacterial cell wall has always been one of the primary targets in combat against pathogens as bacteria quickly become non-viable in the absence of it. The MreB

filamentous system, located beneath the cell membrane has a primary role in cell wall assembly and plays an essential role in directing the peptidoglycan synthase localization and cell wall synthesis. Due to its function of maintaining the cell shape, extensive research is being conducted on the MreB protein and its binding partners, especially on those which can inhibit the primary function of the protein.

A promising way is to combine the inhibitory agents whose synergistic interaction can result in a more powerful antibacterial effect against pathogenic bacteria. In this paper, we investigated the combined effect of the MreB-specific antimicrobial A22, and vancomycin, a widely used antibiotic.

Vancomycin is an effective antibiotic against Gram-positive bacteria like *Enterococcus* and *Streptococcus* species, which are members of the ESKAPEE group of pathogens. The members of this group can 'escape' commonly used antibiotics thanks to their increasing multidrug resistance. The MIC value for these pathogens typically ranges from a few to several tens of μg/ml. Vancomycin is not effective against Gram-negative bacteria and its MIC value (200 μg/ml) is significantly elevated. However, in the case of combined use of vancomycin and A22 - a known small molecule inhibitor of MreB protein - the MIC value decreases dramatically to a value (1.56 μg/ml) which is characteristic for Gram-positive bacteria. This result confirms that the antimicrobial efficacy of vancomycin can be extended to Gram-negative bacteria if it is administered together with A22.

To investigate the effect of vancomycin on cell shape and intracellular distribution of MreB filaments, A22 combined with fluorescently labelled Bodipy-vancomycin was used. In our observation, Bodipy-vancomycin appears not only beneath the cell wall according to the fluorescent microscopy measurements, but the shape of the cells changes from rod-like to spherical. It means that in the presence of A22 the entry of vancomycin into the *E. coli* cell is strongly promoted. The exact mechanism by which vancomycin can enter *E. coli* is not known yet; the change in the structure of the cell wall caused by A22 can facilitate the entrance. This finding leads us to the conclusion that A22 and vancomycin have a synergistic interaction with each other, meaning that their combined antibacterial effect increases considerably by low applied concentrations. It can be concluded that vancomycin treatment can also be extended to infections caused by not only Gram-positive but by Gram-negative bacteria without increasing the concentration of the antibiotic, when used in combination with low-concentration A22. MreB-vancomycin binding can occur at serum vancomycin concentrations developed during antibiotic treatment.

As previously described, vancomycin is unable to penetrate the membranes of *E.coli* cells. However, in the presence of A22, vancomycin finds its way into the intracellular space and according to our observations, binds directly to the MreB filamentous network beneath the cell wall. A22 diffuses into the cell and disrupts the cell wall synthesis and other cell functions, resulting in cell death. The combined application of A22 and vancomycin enhances this progression, suggesting a strong synergistic interaction between them. Direct binding of vancomycin to MreB filaments can cause intra- and/or interfilamental structural changes, as confirmed by fluorescent anisotropy and intensity measurements. In addition to its clinical relevance, fluorescently labelled vancomycin-MreB (in our study Bodipy-vancomycin-MreB) offers technological advantages as well, as it significantly facilitates the visualization of the spatial distribution of the MreB protein within. Although our data clearly show the synergistic interaction of A22 and vancomycin on the MreB monomer/filament, this question needs further investigation.

Using *in silico* docking experiments, we aimed to identify the binding site(s) of vancomycin on MreB filament to elucidate whether the binding sites of A22, the nucleotide and vancomycin interfere with each other. A22 is known to inhibit the function of MreB by stopping the nucleotide hydrolysis by blocking the inorganic phosphate (P_i) release. In solution there is an equilibrium between the

511 monomeric and dimeric form of vancomycin. The docking calculations clarified that both forms of
512 vancomycin can interact with the modelled MreB dimer at distinct binding sites (Site1 nor Site2). In
513 both cases, vancomycin showed to adapt a bridging position thus stabilizing the filament. The binding
514 site of A22 and ADP has been experimentally determined for MreB from *Caulobacter vibrioides*.
515 Superposing the structures of MreB *Thermotoga maritima* and *Caulobacter vibrioides* vancomycin
516 binding sites (neither Site1 nor Site2) do not overlap of the A22 or nucleotide binding pockets. These
517 well separated binding sites allow the action of A22 and vancomycin to act in simultaneously on the
518 MreB filament. These spatially distanced binding sites provide a structural basis for their synergistic
519 effect.

520 Our results are consistent with the currently emerging trend that the synergism between two or more
521 drug molecules may be a potential solution to the urgent problem of antibiotic resistance.

522

Conflict of Interest

The authors declare that the research was conducted in the absence of any commercial or financial relationships that could be construed as a potential conflict of interest.

Author Contributions

- Conceptualization: SB, EB, MN
- Methodology & Investigation: TJ, GM, RB, CH, ZG
- Analysis: EB, TH, BL, SB.
- Writing & Revision: SB, EB, AL, RB, CH
- Supervision & Administration: SB

Funding

The research in Hungary was funded by NKFIH within the framework of the TKP2021-EGA-17 project.
A.L. acknowledges funding from the Hungarian National Research and Innovation Office (K-137557) and 2024-1.2.3-HU-RIZONT-2024-00063.
The research was performed in "István Ábrahám'' Nano-Bio-Imaging Core Facility, University of Pécs.
We acknowledge KIFÜ (Governmental Agency for IT Development, Hungary) for awarding us access to the Komondor HPC facility based in Hungary.
The paper was supported by the János Bolyai Research Scholarship of the Hungarian Academy of Sciences (R. Börzsei BO/00620/24/5).

Data Availability Statement

Data available on request from the authors.

References

Awuni, E. (2020). Status of Targeting MreB for the Development of Antibiotics. *Frontiers in Chemistry* 7. doi: 10.3389/fchem.2019.00884

Awuni, Y., Jiang, S., Robinson, R. C., and Mu, Y. (2016). Exploring the A22-Bacterial Actin MreB Interaction through Molecular Dynamics Simulations. *J. Phys. Chem. B* 120, 9867–9874. doi: 10.1021/acs.jpcb.6b05199

Bean, G. J., Flickinger, S. T., Westler, W. M., McCully, M. E., Sept, D., Weibel, D. B., et al. (2009). A22 disrupts the bacterial actin cytoskeleton by directly binding and inducing a low-affinity state in MreB. *Biochemistry* 48, 4852–7. doi: 10.1021/bi900014d

Berman, H. M., Westbrook, J., Feng, Z., Gilliland, G., Bhat, T. N., Weissig, H., et al. (2000). The Protein Data Bank. *Nucleic Acids Res* 28, 235–242. doi: 10.1093/nar/28.1.235

Bonez, P. C., Ramos, A. P., Nascimento, K., Copetti, P. M., Souza, M. E., Rossi, G. G., et al. (2016). Antibacterial, cyto and genotoxic activities of A22 compound ((S-3, 4 -dichlorobenzyl) isothiourea hydrochloride). *Microbial Pathogenesis* 99, 14–18. doi: 10.1016/j.micpath.2016.07.007

Braun, J., Eckes, S., Rommens, P. M., Schmitz, K., Nickel, D., and Ritz, U. (2020). Toxic Effect of Vancomycin on Viability and Functionality of Different Cells Involved in Tissue Regeneration. *Antibiotics (Basel)* 9, 238. doi: 10.3390/antibiotics9050238

Bryan, E. J., Sagong, H. Y., Parhi, A. K., Grier, M. C., Roberge, J. Y., LaVoie, E. J., et al. (2022). TXH11106: A Third-Generation MreB Inhibitor with Enhanced Activity against a Broad Range of Gram-Negative Bacterial Pathogens. *Antibiotics* 11, 693. doi: 10.3390/ANTIBIOTICS11050693

Clinical and Laboratory Standards Institute ed. (2015). *Methods for dilution antimicrobial susceptibility tests for bacteria that grow aerobically: M07-A10 ; approved standard*., 10. ed. Wayne, PA: Committee for Clinical Laboratory Standards.

Ent, F. van den, Amos, L. a, and Löwe, J. (2001). Prokaryotic origin of the actin cytoskeleton. *Nature* 413, 39–44. doi: 10.1038/35092500

Ent, F. van den, Izoré, T., Bharat, T. A. M., Johnson, C. M., and Löwe, J. (2014). Bacterial actin MreB forms antiparallel double filaments. *eLife* 2014, 1–22. doi: 10.7554/eLife.02634

Hall, S., Grayson, J., Grant, G., Vertullo, C., and Anoopkumar-Dukie, S. (2024). In Vitro Evaluation of Vancomycin-Induced Toxicity in Human Primary Knee Chondrocytes. *Int J Toxicol* 43, 177–183. doi: 10.1177/10915818231216413

Huey, R., Morris, G. M., Olson, A. J., and Goodsell, D. S. (2007). A semiempirical free energy force field with charge-based desolvation. *J Comput Chem* 28, 1145–1152. doi: 10.1002/jcc.20634

INTRAVENOUS VANCOMYCIN DOSING AND MONITORING GUIDELINES (n.d.).

James, C. W., and Gurk-Turner, C. (2001a). Recommendations for monitoring serum vancomycin concentrations. *Proc (Bayl Univ Med Cent)* 14, 189–190. doi: 10.1080/08998280.2001.11927763

James, C. W., and Gurk-Turner, C. (2001b). Recommendations for monitoring serum vancomycin concentrations. *Proc (Bayl Univ Med Cent)* 14, 189–190. Available at: https://www.ncbi.nlm.nih.gov/pmc/articles/PMC1291340/ (Accessed July 27, 2023).

Kang, H.-K., and Park, Y. (2015). Glycopeptide Antibiotics: Structure and Mechanisms of Action. *J Bacteriol Virol* 45, 67–78. doi: 10.4167/jbv.2015.45.2.67

Kitzis, M. D., and Goldstein, F. W. (2006). Monitoring of vancomycin serum levels for the treatment of staphylococcal infections. *Clinical Microbiology and Infection* 12, 92–95. doi: 10.1111/j.1469-0691.2005.01306.x

Kotzialampou, A., Protonotariou, E., Skoura, L., and Sivropoulou, A. (2021). Synergistic Antibacterial and Antibiofilm Activity of the MreB Inhibitor A22 Hydrochloride in Combination with Conventional Antibiotics against *Pseudomonas aeruginosa* and *Escherichia coli* Clinical Isolates. *International Journal of Microbiology* 2021, e3057754. doi: 10.1155/2021/3057754

Krul, D., Negoseki, B. R. da S., Siqueira, A. C., Tomaz, A. P. de O., dos Santos, É. M., de Sousa, I., et al. (2025). Spread of antimicrobial-resistant clones of the ESKAPEE group: From the clinical setting to hospital effluent. *Science of The Total Environment* 973, 179124. doi: 10.1016/j.scitotenv.2025.179124

Kumar, A., Kukal, S., Marepalli, A., Kumar, S., Govindarajan, S., and Pramanik, D. (2024). Probing the Molecular Interactions of A22 with Prokaryotic Actin MreB and Eukaryotic Actin: A Computational and Experimental Study. 2024.04.27.591468. doi: 10.1101/2024.04.27.591468

Levin, P. A., Margolis, P. S., Setlow, P., Losick, R., and Sun, D. (1992). Identification of Bacillus subtilis genes for septum placement and shape determination. *J Bacteriol* 174, 6717–6728. doi: 10.1128/jb.174.21.6717-6728.1992

Longauer, B., Bódis, E., Lukács, A., Barkó, S., and Nyitrai, M. (2022). Solubility and Thermal Stability of Thermotoga maritima MreB. *International Journal of Molecular Sciences* 23, 16044. doi: 10.3390/ijms232416044

Martin, J. H., Norris, R., Barras, M., Roberts, J., Morris, R., Doogue, M., et al. (2010). Therapeutic Monitoring of Vancomycin in Adult Patients: A Consensus Review of the American Society of Health-System Pharmacists, the Infectious Diseases Society of America, and the Society of Infectious Diseases Pharmacists. *Clin Biochem Rev* 31, 21–24. Available at: https://www.ncbi.nlm.nih.gov/pmc/articles/PMC2826264/ (Accessed July 27, 2023).

Morris, G. M., Huey, R., Lindstrom, W., Sanner, M. F., Belew, R. K., Goodsell, D. S., et al. (2009). AutoDock4 and AutoDockTools4: Automated docking with selective receptor flexibility. *Journal of Computational Chemistry* 30, 2785–2791. doi: 10.1002/jcc.21256

Muheim, C., Götzke, H., Eriksson, A. U., Lindberg, S., Lauritsen, I., Nørholm, M. H. H., et al. (2017). Increasing the permeability of Escherichia coli using MAC13243. *Sci Rep* 7, 17629. doi: 10.1038/s41598-017-17772-6

Nicholson, A., Perry, J. D., James, A. L., Stanforth, S. P., Carnell, S., Wilkinson, K., et al. (2012). In vitro activity of S-(3,4-dichlorobenzyl)isothiourea hydrochloride and novel structurally related compounds against multidrug-resistant bacteria, including Pseudomonas aeruginosa and Burkholderia cepacia complex. *International Journal of Antimicrobial Agents* 39, 27–32. doi: 10.1016/j.ijantimicag.2011.08.015

620 Nyilasi, I., Kocsubé, S., Krizsán, K., Galgóczy, L., Papp, T., Pesti, M., et al. (2014). Susceptibility of clinically
621 important dermatophytes against statins and different statin-antifungal combinations. *Med Mycol* 52,
622 140–148. doi: 10.3109/13693786.2013.828160

623 Perin, N., Roger, C., Marin, G., Molinari, N., Evrard, A., Lavigne, J.-P., et al. (2020). Vancomycin Serum
624 Concentration after 48 h of Administration: A 3-Years Survey in an Intensive Care Unit. *Antibiotics* 9,
625 793. doi: 10.3390/antibiotics9110793

626 Sagong, H. Y., Rosado-Lugo, J. D., Bryan, E. J., Ferrer-Gonzalez, E., Wang, Y., Cao, Y., et al. (2022). Novel MreB
627 Inhibitors with Antibacterial Activity Against Gram (-) Bacteria. In Review. doi: 10.21203/rs.3.rs-
628 1824695/v1

629 Schäfer, M., Schneider, T. R., and Sheldrick, G. M. (1996). Crystal structure of vancomycin. *Structure* 4, 1509–
630 1515. doi: 10.1016/s0969-2126(96)00156-6

631 Schrödinger, LLC (2015). The PyMOL Molecular Graphics System, Version 1.8.

632 Stewart, J. J. P. (2013). Optimization of parameters for semiempirical methods VI: more modifications to the
633 NDDO approximations and re-optimization of parameters. *J Mol Model* 19, 1–32. doi:
634 10.1007/s00894-012-1667-x

635 Strahl, H., Bürmann, F., and Hamoen, L. W. (2014). The actin homologue MreB organizes the bacterial cell
636 membrane. *Nature communications* 5, 1–11. doi: 10.1038/ncomms4442

637 Varley, A. W., and Stewart, G. C. (1992). The divIVB region of the Bacillus subtilis chromosome encodes
638 homologs of Escherichia coli septum placement (minCD) and cell shape (mreBCD) determinants. *J*
639 *Bacteriol* 174, 6729–6742. doi: 10.1128/jb.174.21.6729-6742.1992

640 White, C. L., and Gober, J. W. (2012). MreB: pilot or passenger of cell wall synthesis? *Trends in Microbiology*
641 20, 74–79. doi: 10.1016/j.tim.2011.11.004

642 World Health Organization (2025). *The selection and use of essential medicines, 2025: WHO Model List of*
643 *Essential Medicines, 24th list*. World Health Organization. doi: 10.2471/B09474

644